Experience-dependent regulation of CaMKII activity within single visual cortex synapses in vivo

Amanda F. Mower[a,1], Showming Kwok[a,b,1], Hongbo Yu[a,2], Ania K. Majewska[a,3], Ken-Ichi Okamoto[a,b,4], Yasunori Hayashi[a,b,c,5], and Mriganka Sur[a,5]

[a]The Picower Institute for Learning and Memory, Department of Brain and Cognitive Sciences, Massachusetts Institute of Technology, Cambridge, MA 02139; [b]RIKEN–MIT Neuroscience Research Center, Massachusetts Institute of Technology, Cambridge, MA 02139; and [c]Brain Science Institute, RIKEN, Wako, Saitama 351-0198, Japan

Edited* by Jon H. Kaas, Vanderbilt University, Nashville, TN, and approved November 10, 2011 (received for review May 23, 2011)

Unbalanced visual input during development induces persistent alterations in the function and structure of visual cortical neurons. The molecular mechanisms that drive activity-dependent changes await direct visualization of underlying signals at individual synapses in vivo. By using a genetically engineered Förster resonance energy transfer (FRET) probe for the detection of CaMKII activity, and two-photon imaging of single synapses within identified functional domains, we have revealed unexpected and differential mechanisms in specific subsets of synapses in vivo. Brief monocular deprivation leads to activation of CaMKII in most synapses of layer 2/3 pyramidal cells within deprived eye domains, despite reduced visual drive, but not in nondeprived eye domains. Synapses that are eliminated in deprived eye domains have low basal CaMKII activity, implying a protective role for activated CaMKII against synapse elimination.

cortical circuits | ocular dominance plasticity | spines | excitatory synaptic transmission | serine/threonine protein kinase

During a developmental critical period, alteration of neuronal responses in the visual cortex can occur after brief periods of monocular deprivation (MD) (1–3). These alterations are mediated by sequential mechanisms that transduce changes in the amount and pattern of visual activity from the two eyes to changes in synaptic drive (4–6). Thus, the initial loss of responses from the closed eye is known to be rapid, on the order of hours, as detailed elsewhere in PNAS (7), and mediated by mechanisms that implement synaptic depression. The gain of responses from the open eye is thought to be slower, on the order of days, and mediated by homeostatic scaling of responses as well as homosynaptic long-term potentiation (LTP)-like mechanisms (8–15), although rapid gain of responses on the order of hours also occurs (7). However, the structural and molecular basis for these changes at the level of single synapses are not fully understood (16–20). Two important reasons are that the precise location and distribution of synapses undergoing changes in the intact brain, and the specific molecular transformations that occur at these synapses during experience-dependent plasticity, are unknown.

Excitatory neurons in layer 2/3 receive synaptic inputs from multiple sources, including feedforward, local, and long-range intracortical axons (Fig. 1*A*), and exhibit rapid functional changes following even brief MD (1–3). MD is known to reduce the effectiveness of deprived eye-driven synapses as well as rapidly eliminate synapses (16, 18). However, significant proportions of synapses within deprived eye domains are also preserved after MD, and these synapses, depending on their origin, serve multiple functions: potentiating open eye responses (8, 12), acting as a scaffold for experience-dependent traces and accelerated shifts in response to MD, or enabling recovery of drive when the deprived eye is reopened (7, 12). Thus, understanding why some synapses are lost while others are preserved after MD, and the mechanistic differences between these sets of synapses, remains an important issue to be resolved.

To address these questions, we developed a method to visualize the effects of MD within identified synapses in vivo based on activation of CaMKII, a protein kinase that is necessary and sufficient for the induction and maintenance of synaptic plasticity (21–23). By expressing a FRET-based optical probe for CaMKII in neurons of the primary visual cortex (V1) in ferrets, and imaging individual spines within deprived or nondeprived eye zones in vivo before and after a period of MD, we demonstrate distinct differences between synapses that are lost and those that are preserved. Spines that are lost after MD have low basal levels of CaMKII, whereas spines that are preserved show increased activation of CaMKII following MD. These data indicate that CaMKII activation after MD could constitute a major difference between lost vs. preserved synapses, and suggest that rapid CaMKII activation represents a potential mechanism for synapse preservation following reduction of input drive.

Results

A FRET-based optical probe (24) known as Camui (Fig. 1*B*), in combination with in vivo two-photon laser scanning microscopy and intrinsic signal optical imaging in ferret visual cortex (Fig. 1*C* and Fig. S1*E*), enabled us to detect changes in CaMKII activity within individual spines in functionally identified regions of cortex before and after manipulation of visual drive. The emission fluorescence spectrum of unstimulated Camui expressed in HEK293 cells showed FRET, as evidenced by the presence of a YFP emission peak under CFP specific excitation (Fig. S1*A*). Upon Ca^{2+} stimulation, the YFP peak decreased whereas the CFP peak was dequenched. Chelating Ca^{2+} only partially reversed this change. The remaining change was attributable to autophosphorylation at threonine (T) 286 (24). Camui with a mutation of T305 and T306 to aspartate (D) is deficient in Ca^{2+}/calmodulin binding (25, 26), and, as expected, showed no response to Ca^{2+} stimulation (Fig. S1 *B* and *D*). Therefore, the change in FRET, or change in CFP/YFP ratio, is a reliable indicator of CaMKII activation (Fig. S1 *A*–*D*).

Author contributions: A.F.M., S.K., Y.H., and M.S. designed research; A.F.M., S.K., H.Y., and A.K.M. performed research; K.-I.O. contributed new reagents/analytic tools; A.F.M., S.K., H.Y., A.K.M., and Y.H. analyzed data; and A.F.M., S.K., Y.H., and M.S. wrote the paper.

The authors declare no conflict of interest.

*This Direct Submission article had a prearranged editor.

[1]A.F.M. and S.K. contributed equally to this work.

[2]Present address: Center for Brain Science Research and School of Life Sciences, Fudan University, Shanghai 200433, China.

[3]Present address: Department of Neurobiology and Anatomy, University of Rochester, NY 14642.

[4]Present address: Samuel Lunenfeld Research Institute, Mount Sinai Hospital, Toronto, ON, Canada M5G 1X5.

[5]To whom correspondence may be addressed. E-mail: yhayashi@brain.riken.jp or msur@mit.edu.

This article contains supporting information online at www.pnas.org/lookup/suppl/doi:10.1073/pnas.1108261109/-/DCSupplemental.

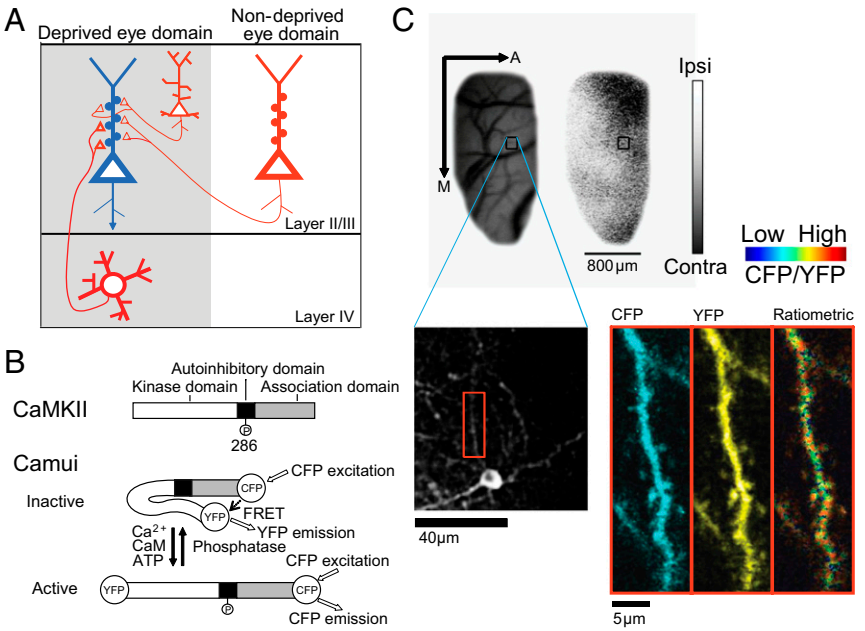

Fig. 1. Imaging of CaMKII activity in identified OD domains. (*A*) Schematic diagram of a sample pyramidal neuron (blue) in layer II/III within the deprived eye domain receiving inputs from multiple sources (red). Thick red triangles represent feedforward synapses. Other synapses derive from local and longer-range axons, including inputs from the nondeprived eye. (*B*) *Top*: Schematic drawing of the CaMKII protein. *Bottom*: Conformations of Camui in the inactive and active form. (*C*) Alignment of two-photon microscopic images with OD map. Blood vessel and OD maps were obtained using intrinsic signal optical imaging (*Upper*: A, anterior; M, medial). Gray scale indicates ODI (white, ipsilateral eye dominated; black, contralateral eye dominated). Blood vessels in low-magnification optical and two-photon microscopic images were used to align two-photon images (*Lower*) to OD domains. A dendritic segment (red box) is magnified (*Right*) and displayed as channel separated images (CFP and YFP) as well as a ratiometric image in intensity-modulated display mode, indicating the CFP/YFP ratio. Warm hue represents high CaMKII activity.

To monitor the activity of CaMKII associated with visual cortical plasticity, we expressed Camui in V1 neurons in ferrets by using an HSV vector during the critical period, and repeatedly imaged the neurons in vivo through a cranial window before and after 4 h of MD, a manipulation known to cause functional changes in neurons of ferret V1 (7). To precisely align imaged spines with functional domains driven by the ipsilateral or contralateral eye, the fluorescence image of spines and dendrites obtained by two-photon imaging was matched to the ocular dominance (OD) map obtained by intrinsic signal optical imaging using the common blood vessel patterns obtained with both techniques (Fig. 1*C* and Fig. S1*E*). To examine overall trends, we first pooled data from spines that lay within deprived [OD index (ODI) < −0.1], binocular (−0.1 ≤ ODI ≤ −0.1), or nondeprived (ODI > 0.1) eye domains. CaMKII activity showed a significant increase in both spines (Fig. 2*A*) and adjacent dendritic regions (Fig. S2*A*) in deprived eye domains after 4 h MD [Kolmogorov–Smirnov (KS) test, $P < 0.05$ for spines and dendrites]. CaMKII activity did not increase in the binocular domain in dendritic spines, although there was a slight tendency (KS test, $P = 0.096$; Fig. 2*B*). Within the nondeprived eye domain, CaMKII activity did not show a significant change in spines or dendritic regions (KS test, $P = 0.443$ for spines and $P = 0.916$ for dendritic regions; Fig. 2*C* and Fig. S2*C*).

An increase in CaMKII activation in spines within a region with reduced afferent drive was unexpected from in vitro studies, in which increased CaMKII is correlated with the induction of LTP and its maintenance via insertion of AMPA receptors at potentiated synapses (21, 27, 28). In light of potentially confounding variables such as changes in cerebral blood flow, level of blood oxygenation, and the differential cortical scattering of fluorescence, we repeated the same experiments using two different negative control probes that would not be expected to show a CaMKII-dependent FRET change: Camui-T305D/T306D mutant (Fig. S1*B*) and a CFP-YFP (C-Y) direct fusion protein (Fig. S1*C*). Neither probe produced a FRET change following MD (T305D/T306D mutant, KS test, $P = 0.658$ for spines and $P = 0.953$ for dendritic regions; fusion, KS test, $P = 0.811$ for spines and $P = 0.936$ for dendritic regions; Fig. 2*D* and Fig. S2*D*).

Pooling all spines from each site as comprising a single observation, we found a significant inverse correlation between the ODI and normalized change in CFP/YFP ratio (Pearson correlation coefficient $R = -0.65$; $P < 0.05$, paired t test; Fig. 2*E*). In the deprived eye domains, there was an increase in synaptic CaMKII activity, whereas in the nondeprived eye domains, there was little or no change. Dendritic regions followed the same tendency (Fig. S2*E*). Negative control constructs fell outside of this correlation, showing almost no change in CFP/YFP ratio, confirming that the observed changes in FRET are specific to activation of CaMKII following 4 h MD.

Next, we examined whether the activation of CaMKII observed in the deprived eye domains was related to the predeprivation state of the synapse. Each spine in the deprived eye domain was rank-ordered according to its basal CFP/YFP ratio, from highest to lowest, and plotted together with its ratio after 4 h MD (Fig. 3*A*). Basal and 4 h MD CaMKII activity data were binned in 20% increments and compared with each other at each level. Basal CaMKII activity varied considerably; however, there was a clear tendency for spines that had high basal CaMKII activity to show a decrease in CaMKII activity following 4 h MD ($P < 0.05$, paired two-tailed t test; Fig. 3*B*, first bin). In contrast, spines with moderate to low basal CaMKII activity showed an increase ($P < 0.05$, $P < 0.05$, and $P < 0.05$; Fig. 3*B*, third to fifth bins). Analysis of dendritic regions adjacent to these spines showed similar results (Fig. S3). In the binocular domain, although we did not see a statistically significant change in averaged CaMKII activity (Fig. 2 *B* and *D*), we observed a similar tendency at individual spine level, namely spines with high

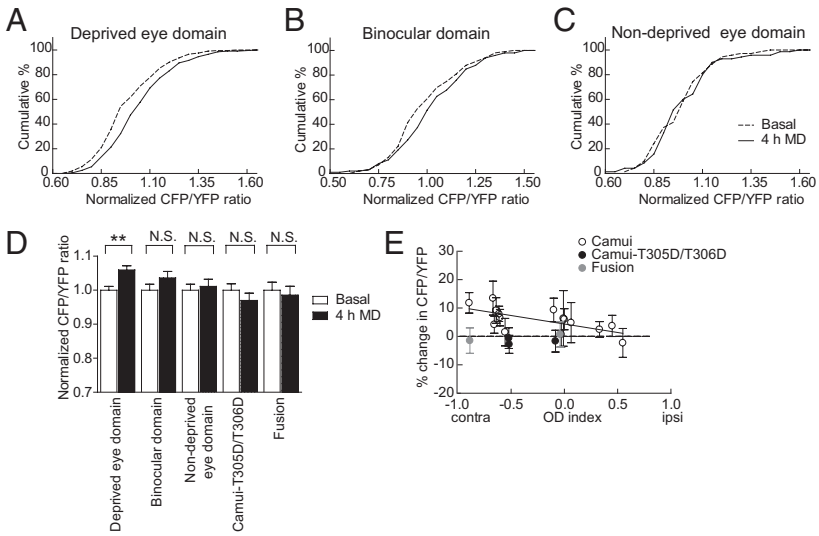

Fig. 2. Changes in synaptic CaMKII activity in spines within different eye domains after 4 h MD. (*A–C*) CaMKII activity of individual synapses in (*A*) deprived eye domains (ODI < −0.1, *n* = 201 spines from seven imaging sites), (*B*) binocular domains (−0.1 ≤ ODI ≤ 0.1, *n* = 99 spines from five imaging sites), and (*C*) nondeprived domains (ODI > 0.1, *n* = 70 spines from three imaging sites) before (basal) and after 4 h MD. CFP/YFP ratios of individual spines normalized to the average basal CFP/YFP ratio of all spines within the respective imaged cortical site are plotted. (*D*) Bars show mean values of data pooled from each site imaged in individual animals, including data from negative control constructs: Camui-T305D/T306D (*n* = 98 spines from three imaging sites) and C-Y fusion protein (*n* = 33 spines from two imaging sites). $^{**}P < 0.05$ (KS test); N.S., nonsignificant. (*E*) Mean percent change in FRET within spines in each imaging site shown in *A–C*, including negative control data sites pooled in *D*, plotted versus their respective ODI value (*R* = −0.65). Error bars represent SEM within each imaging site.

CaMKII activity tended to decrease after MD whereas those with lower CaMKII activity increased (Fig. 3 *C* and *D*). In contrast, in the open eye domain where visual input remains unchanged, this tendency was observed in only the last bin (Fig. 3 *E* and *F*). Thus, the basal level of CaMKII acted as an indicator of the direction of change after MD in domains that had deprived visual input, with most spines showing an increase in activity and a few showing a decrease.

A key correlate of MD is spine elimination: the majority of spines in deprived eye zones persisted after short periods of MD, whereas a subset of spines was eliminated (16, 18). We wondered if there was a common feature among lost spines. We found that a small but reliable fraction of spines (seven of 116 spines) within four deprived eye sites were eliminated following 4 h MD (Fig. 4*A*). This loss after only 4 h of MD is consistent with the spine loss described in the companion study in PNAS (ref. 7, see also *Discussion*). Interestingly, the basal CaMKII activity of these eliminated spines was lower than the average CaMKII activity of other spines in the same imaged cortical site ($P < 0.05$, paired two-tailed *t* test; Fig. 4*B*). In contrast, spines within these same cortical sites that were not eliminated had CaMKII activity that remained high or increased after 4 h MD. Furthermore, dendritic regions adjacent to eliminated spines, and spines that persisted after 4 h MD, had basal CaMKII activity levels comparable to the average activity of adjacent dendritic regions ($P > 0.05$, paired two-tailed *t* test; Fig. 4*C*). Only one spine in the binocular domain, and two in the open eye domain, were determined to be eliminated at 4 h MD. This observation aligns with the findings of the companion paper (7) in which spine loss was significantly lower within the binocular domain compared with the closed eye domain (figure 6c of ref. 7). Combined, synapses with low CaMKII activity follow one of two fates: a majority of spines gain CaMKII activity after MD and persist, whereas a minority are eliminated. The eliminated spines consistently have lower CaMKII activity than the average, but not all spines with low CaMKII activity are removed.

We found no correlation between spine size and basal CaMKII activity ($R = 0.11$; $P > 0.05$, two-tailed *t* test; Fig. 5*A*). There was also no correlation between the initial size of a spine and the change in CFP/YFP ratio that resulted after 4 h MD ($R = 0.08$; $P > 0.05$, two-tailed *t* test; Fig. 5*B*), indicating that spine size was not a determinant of basal CaMKII activity levels or of the change in CFP/YFP ratio after MD. Additionally, changes in CaMKII activity were not correlated with relative cortical depth of spines or dendritic regions (Fig. S4).

Discussion

We have overcome the technical challenges of performing chronic in vivo two-photon microscopy of a FRET probe in single synapses in ferret V1. In contrast to in vivo imaging of a single fluorophore, ratiometric imaging of our two-fluorophore FRET probe has allowed us to visualize changes in the activity of a molecular correlate of synaptic plasticity in vivo during short-term changes in visual drive. Alignment of these ratiometric images with identified functional domains in the visual cortex further allowed us to define the location of these single synapses to deprived, binocular, and nondeprived eye regions. These technical advances open the door for detailed analysis of molecular correlates and signaling pathways of plasticity processes in vivo.

We observed eye-domain specific CaMKII activity changes, specifically an overall increase in CaMKII activity in deprived but not nondeprived eye domains. This was the result of an increase in CaMKII activity in the majority of spines with moderate to low levels of basal CaMKII activity and a reduction in a few spines with high basal CaMKII activity. In addition, spines that were eliminated constituted a subset of spines with low basal CaMKII activity. The observation that not all spines with low basal CaMKII activity are eliminated indicates that (*i*) low basal CaMKII activity is a prerequisite for elimination but is not sufficient, and (*ii*) there might be additional mechanisms that also participate in the regulation of this important step of spine removal. These changes in CaMKII activation in deprived zones are consistent with the physiological consequences of MD and indeed predict their structural basis. The initial rapid reduction of drive from the deprived eye after MD is accompanied by a rapid but small increase of drive from the nondeprived eye (7), followed by a slower increase of functional drive and anatomical

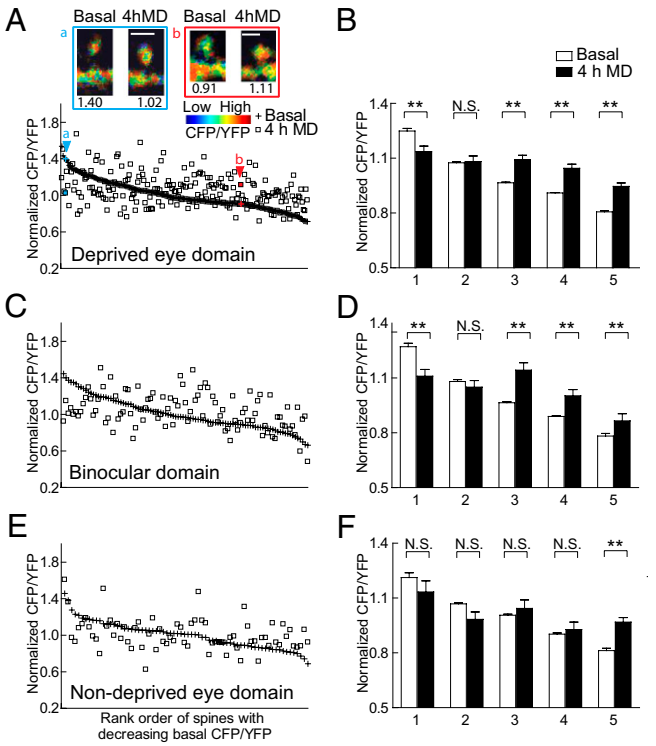

Fig. 3. CaMKII activation increases in deprived domain spines with low to moderate basal CaMKII activity and decreases in spines with high basal CaMKII activity. (*A*) *Bottom*: Normalized basal CFP/YFP ratios from individual spines in the deprived eye domain are ranked and plotted in decreasing order along with their respective CFP/YFP ratio after 4 h MD. *Top*: Intensity modulated display images of a spine with high basal and lower CaMKII activity after 4 h MD (*A*) as well as a spine with low basal and higher CaMKII activity level after 4 h MD (*B*). Spines *a* and *b* are indicated by their respective arrowheads in the plot. CFP/YFP values of the spines are shown below their images. (Scale bar: 2 μm.) (*B*) Data from *A* were binned in 20% increments and the mean was plotted. Numbers 1–5 on the *x* axis denote the first to fifth bins (**$P < 0.05$, paired two-tailed *t* test). (*A* and *B*) $n = 201$ spines from seven imaging sites. (*C*–*F*) Normalized spine CFP/YFP ratios in the binocular domain (*C* and *D*) and open eye domain (*E* and *F*) plotted in the same manner as *A* and *B*. (*C* and *D*) $n = 99$ spines from five imaging sites; (*E* and *F*) $n = 70$ spines from three imaging sites. Error bars represent SEM.

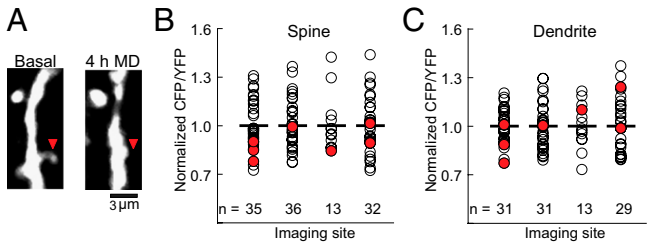

Fig. 4. Spines that are lost following 4 h MD have low basal CaMKII activity. (*A*) Arrowhead shows a dendritic spine that was lost after 4 h MD. (*B*) Distribution of basal CaMKII activity in eliminated and spared spines. Circles represent basal CaMKII activity in individual spines grouped according to imaged cortical site. Only sites which contained eliminated spines are shown. Horizontal bars indicate the population mean CFP/YFP ratio of each imaged cortical site. Red circles indicate spines that were eliminated after 4 h MD. White circles indicate spines that persisted after 4 h MD (*n* indicates spine number, including spines that disappeared, in each imaged region; seven out of a total of 116 spines were eliminated). Eliminated spines have significantly lower basal CFP/YFP ratios ($P < 0.05$, two-tailed *t* test). (*C*) Basal CaMKII activity levels in dendritic regions adjacent to spines that were eliminated were not significantly different from the population mean of their imaging site, shown as in *B* ($P > 0.05$, two-tailed *t* test).

expansion of nondeprived inputs (8, 12, 29, 30). Our data suggest that the rapid loss of deprived eye drive is mediated by Hebbian mechanisms that include (*i*) a loss of some spines, with the lost synapses having lower than average basal levels of CaMKII activity; and (*ii*) a reduction of CaMKII activity at synapses that previously had high basal levels of CaMKII activity. It is likely that feedforward synapses (Fig. 1*A*) constitute a high proportion of this latter set. More interestingly, the loss of deprived eye drive is accompanied by a homeostatic increase of CaMKII activity in the majority of spines that had moderate to low levels of basal CaMKII activity. These spines are preserved following MD; such spines likely form a substrate for response scaling via enhanced drive from the nondeprived eye (Fig. 1*A*), through a delayed process of synaptic potentiation and even reorganization of intracortical presynaptic partners (31, 32). These spines likely also lay a structural trace for an accelerated functional shift of responses following later episodes of deprivation (33).

Our finding of spine loss in the deprived eye domain is consistent with the findings of the companion paper (7) and indeed provides a mechanism by which an activity-dependent rule for spine loss and preservation following MD may be implemented. The magnitude of spine loss in this study, however, is lower than that in the companion study (7). This disparity might be explained by several factors: (*i*) small mismatches in the OD regions that were examined in the present and companion study (7); (*ii*) overexpression of CaMKII might protect spines from being eliminated; (*iii*) the possibility that the effect of spine loss ramps up between 4 h of MD (present study) and 6 h (companion study, ref. 7); and (*iv*) the spines analyzed in the present study were selected conservatively and represented the most prominent and best labeled spines, as a result of the FRET images being dimmer than the GFP labeling in the companion study (7).

In addition, our data suggest that CaMKII activity increased more in binocular dendritic domains (Fig. S2*C*) than in spines. It is known that CaMKII has an active mechanism for being translocated and retained in the dendritic spine in an activity-dependent fashion (e.g., interaction with the NR2B subunit of

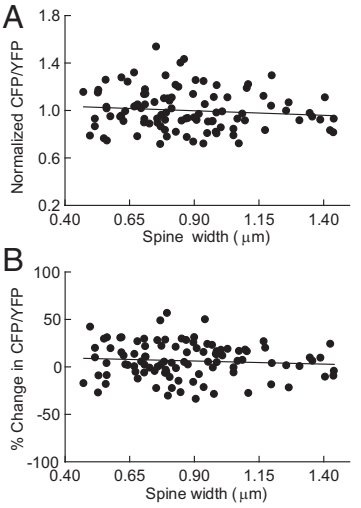

Fig. 5. Basal CaMKII activity and changes in CaMKII activity following 4 h MD are not correlated with spine size. (*A*) Basal CFP/YFP ratio in individual spines plotted against spine width. (*B*) Percent change in CFP/YFP ratio in individual spines after 4 h MD plotted against spine width. Spines shown ($n = 100$) are from deprived eye sites with same image brightness.

the NMDA receptor or self-association) (34, 35). A typical LTP-inducing stimulus effectively recruits this mechanism, allowing CaMKII to be retained at the synapse (36). However, it is not known how CaMKII behaves in response to a stimulus of intermediate intensity. One possible scenario is that CaMKII is partially activated but cannot be retained at the synapse and thus diffuses away from the synapse into the shaft. This is a possible reason for the difference in activity of CaMKII in the dendritic spine and shaft. The finding that high CaMKII activity within spines, either basally or as a consequence of up-regulation after MD, preserves and stabilizes synapses provides insight into previous reports of the role of CaMKII in synaptic and network plasticity. αCaMKII-T286A mutant mice show deficits in response strengthening of the nondeprived eye in visual cortex following MD (22) and of spared whiskers in barrel cortex after whisker trimming (37). This is consistent with the proposal that CaMKII activity is a critical component of a homeostatic response to reduction of afferent drive that mediates response scaling of spared inputs, and indeed, with CaMKII autophosphorylation having a key role in the induction and maintenance of LTP (21, 27, 28); we predict that, in sensory cortex in vivo, such a role involves nondeprived or spared inputs on neurons in deprived zones. Furthermore, αCaMKII-T286A mutant mice show no increase in stabilization or persistence of new spines in barrel column borders after whisker trimming (38), consistent with the proposal that CaMKII activation is critical for the preservation and maintenance of spines that anchor functional plasticity.

Different molecular mechanisms have been proposed to underlie regulation of synaptic strength in neurons within different functional domains (4, 6, 12, 39). However, it is still not known how these kinds of plasticity at different synapses are linked, and what the molecular targets of these regulatory rules might be (40, 41). Our findings demonstrate that plasticity processes governing synaptic changes as a result of altered drive converge at least partly onto a specific kinase, CaMKII, and that different basal levels of CaMKII in individual synapses can lead to a predictable change in subsequent CaMKII activation levels following an alteration of afferent drive. Thus, modulation of CaMKII activity may be one mechanism by which dynamic changes in activity from multiple sources are coordinated within a neuron.

Materials and Methods

All experiments were performed according to protocols approved by the Massachusetts Institute of Technology Animal Care and Use Committee and conformed to National Institutes of Health guidelines.

Construction of Camui and Controls. We extensively improved and characterized a FRET CaMKII activity probe, Camui (24), resulting in a new version used in this study. The donor and acceptor of Camui were replaced with monomeric [alanine 206 to lysine mutation (42)] Cerulean (43) and monomeric Ypet (44) to prevent aggregation and improve brightness, as required for in vivo imaging. For simplicity, this new version was not assigned a new name because its optical properties are similar to the original version. Camui, Camui-T305D/T306D mutant, and a C-Y direct fusion protein were packaged into HSV as described previously (45).

Characterization of Camui and Its Mutants in Infected HEK239T Cell Lysate. HEK239T cells were infected with HSV-Camui, HSV-Camui-T305D/T306D, and HSV-C-Y viruses and collected after 24 h. The fluorescent profile was analyzed as described previously (46). Further details are provided in *SI Materials and Methods*.

HSV-Camui Injection and in Vivo Cortical Imaging Through Cranial Window. HSV carrying Camui or negative controls were expressed in male ferrets at the critical period for OD plasticity (postnatal days 42–50). A cranial window was implanted post surgery to allow for multiple imaging sessions. After 2 d of viral expression, the same spines and dendritic segments of the L2/3 pyramidal neurons were imaged before and after MD to capture Camui activity changes by using a custom-built two-photon microscope (17), followed by intrinsic signal optical imaging, performed as described previously (47), to obtain OD. Further details are provided in *SI Materials and Methods*.

Analysis of Two-Photon Microscopy Images. Image analysis was performed using Metamorph (Molecular Devices). Images were separated into CFP and YFP channels. Regions of interest were manually placed on the CFP channel image. After subtracting an adjacent background image area devoid of obvious structure, the integrated fluorescence intensity at the best focal plane (according to the CFP channel) of each manually traced spine, and adjacent dendritic region, was measured for CFP and YFP channel images. The CFP/YFP ratio for each region was calculated to provide a quantitative measurement of CaMKII activity. For calculation of spine width, we used methods described previously (48). The majority of analyzed cells were pyramidal and resided in cortical layer 2/3, as determined by the shape of dendritic arborizations and position of cell body. We also considered that cortical depth may lead to optical scattering of one channel more than the other; however, preliminary experiments showed that imaging depth does not systematically affect the CFP/YFP ratio (Fig. S4).

Analysis of Intrinsic Signal Optical Imaging Data. Four single orientation maps from stimulation of each eye were averaged to obtain a contralateral and ipsilateral eye response map. The contralateral eye map was subtracted from the ipsilateral eye map to generate the OD map. ODI was calculated by $(C - I) / (C + I) \times 1{,}000$ per pixel, as described previously (47).

Determination of OD Value for a Specific Spine Site. Blood vessel maps obtained during intrinsic signal optical imaging and two-photon imaging were used to align the images (Fig. 1*C* and Fig. S1*E*). Based on the blood vessel pattern common to images acquired from optical and two-photon imaging techniques, the location of low-power (1×; 800 × 600 μm) FRET images was identified in the cortex and hence within the corresponding OD map (white rectangle, Fig. S1*E*, *a*). High-power (10×; 80 × 60 μm) FRET images were then aligned within the corresponding 1× FRET image, and the perimeter of this region outlined (Fig. S1*E*, *b*). The 10× image or spine site occupied approximately 6 × 4 pixels in the OD map (Fig. S1*E*, *c*; pixel size ~ 14 μm). The ODI of these pixels were averaged, serving as the ODI of the spines analyzed within this site.

Statistics. Initial data analysis was performed using Microsoft Excel and GraphPad software. Plots were made in GraphPad. Statistical differences in values after 4 h MD were calculated in comparison with their respective basal values with the KS test (http://www.physics.csbsju.edu/stats/KS-test.n.plot_form.html) or a two-tailed paired Student *t* test (with Excel). Pearson correlation coefficients were also calculated in Excel.

ACKNOWLEDGMENTS. We thank Dr. Kayi Lee for facilitating data analysis and Dr. Rachael Neve for HSV packaging. This work was supported by a National Institutes of Health (NIH) postdoctoral fellowship (to A.F.M.), grants from the NIH (to M.S.) and RIKEN, NIH Grant R01DA17310, Grant-in-Aid for Scientific Research (A), Grant-in-Aid for Scientific Research on Innovative Area "Foundation of Synapse and Neurocircuit Pathology," from the Ministry of Education, Culture, Sports, Science, and Technology of Japan (to Y.H.), and by 973 program (2010CB327901) from China (to H.Y.).

1. Mioche L, Singer W (1989) Chronic recordings from single sites of kitten striate cortex during experience-dependent modifications of receptive-field properties. *J Neurophysiol* 62:185–197.
2. Freeman RD, Olson C (1982) Brief periods of monocular deprivation in kittens: Effects of delay prior to physiological study. *J Neurophysiol* 47:139–150.
3. Trachtenberg JT, Trepel C, Stryker MP (2000) Rapid extragranular plasticity in the absence of thalamocortical plasticity in the developing primary visual cortex. *Science* 287:2029–2032.
4. Tropea D, Van Wart A, Sur M (2009) Molecular mechanisms of experience-dependent plasticity in visual cortex. *Philos Trans R Soc Lond B Biol Sci* 364:341–355.
5. Hensch TK (2005) Critical period plasticity in local cortical circuits. *Nat Rev Neurosci* 6: 877–888.
6. Berardi N, Pizzorusso T, Ratto GM, Maffei L (2003) Molecular basis of plasticity in the visual cortex. *Trends Neurosci* 26:369–378.
7. Yu H, Majewska AK, Sur M (2012) Rapid experience-dependent plasticity of synapse function and structure in ferret visual cortex in vivo. *Proc Natl Acad Sci USA* 108: 21240–21245.
8. Frenkel MY, Bear MF (2004) How monocular deprivation shifts ocular dominance in visual cortex of young mice. *Neuron* 44:917–923.
9. Desai NS, Cudmore RH, Nelson SB, Turrigiano GG (2002) Critical periods for experience-dependent synaptic scaling in visual cortex. *Nat Neurosci* 5:783–789.

10. Mrsic-Flogel TD, et al. (2007) Homeostatic regulation of eye-specific responses in visual cortex during ocular dominance plasticity. *Neuron* 54:961–972.
11. Maffei A, Nataraj K, Nelson SB, Turrigiano GG (2006) Potentiation of cortical inhibition by visual deprivation. *Nature* 443:81–84.
12. Kaneko M, Stellwagen D, Malenka RC, Stryker MP (2008) Tumor necrosis factor-α mediates one component of competitive, experience-dependent plasticity in developing visual cortex. *Neuron* 58:673–680.
13. Yazaki-Sugiyama Y, Kang S, Câteau H, Fukai T, Hensch TK (2009) Bidirectional plasticity in fast-spiking GABA circuits by visual experience. *Nature* 462:218–221.
14. Goel A, Lee H-K (2007) Persistence of experience-induced homeostatic synaptic plasticity through adulthood in superficial layers of mouse visual cortex. *J Neurosci* 27: 6692–6700.
15. Kirkwood A, Lee HK, Bear MF (1995) Co-regulation of long-term potentiation and experience-dependent synaptic plasticity in visual cortex by age and experience. *Nature* 375:328–331.
16. Oray S, Majewska A, Sur M (2004) Dendritic spine dynamics are regulated by monocular deprivation and extracellular matrix degradation. *Neuron* 44:1021–1030.
17. Majewska A, Sur M (2003) Motility of dendritic spines in visual cortex in vivo: changes during the critical period and effects of visual deprivation. *Proc Natl Acad Sci USA* 100: 16024–16029.
18. Mataga N, Mizuguchi Y, Hensch TK (2004) Experience-dependent pruning of dendritic spines in visual cortex by tissue plasminogen activator. *Neuron* 44:1031–1041.
19. Tropea D, et al. (2006) Gene expression changes and molecular pathways mediating activity-dependent plasticity in visual cortex. *Nat Neurosci* 9:660–668.
20. Majdan M, Shatz CJ (2006) Effects of visual experience on activity-dependent gene regulation in cortex. *Nat Neurosci* 9:650–659.
21. Lisman J, Schulman H, Cline H (2002) The molecular basis of CaMKII function in synaptic and behavioural memory. *Nat Rev Neurosci* 3:175–190.
22. Taha S, Hanover JL, Silva AJ, Stryker MP (2002) Autophosphorylation of alphaCaMKII is required for ocular dominance plasticity. *Neuron* 36:483–491.
23. Gordon JA, Cioffi D, Silva AJ, Stryker MP (1996) Deficient plasticity in the primary visual cortex of α-calcium/calmodulin-dependent protein kinase II mutant mice. *Neuron* 17:491–499.
24. Takao K, et al. (2005) Visualization of synaptic Ca^{2+}/calmodulin-dependent protein kinase II activity in living neurons. *J Neurosci* 25:3107–3112.
25. Colbran RJ, Soderling TR (1990) Calcium/calmodulin-independent autophosphorylation sites of calcium/calmodulin-dependent protein kinase II. Studies on the effect of phosphorylation of threonine 305/306 and serine 314 on calmodulin binding using synthetic peptides. *J Biol Chem* 265:11213–11219.
26. Rich RC, Schulman H (1998) Substrate-directed function of calmodulin in autophosphorylation of Ca^{2+}/calmodulin-dependent protein kinase II. *J Biol Chem* 273: 28424–28429.
27. Hayashi Y, et al. (2000) Driving AMPA receptors into synapses by LTP and CaMKII: Requirement for GluR1 and PDZ domain interaction. *Science* 287:2262–2267.
28. Sanhueza M, McIntyre CC, Lisman JE (2007) Reversal of synaptic memory by Ca^{2+}/calmodulin-dependent protein kinase II inhibitor. *J Neurosci* 27:5190–5199.
29. Shatz CJ, Stryker MP (1978) Ocular dominance in layer IV of the cat's visual cortex and the effects of monocular deprivation. *J Physiol* 281:267–283.
30. Antonini A, Fagiolini M, Stryker MP (1999) Anatomical correlates of functional plasticity in mouse visual cortex. *J Neurosci* 19:4388–4406.
31. Trachtenberg JT, Stryker MP (2001) Rapid anatomical plasticity of horizontal connections in the developing visual cortex. *J Neurosci* 21:3476–3482.
32. Ruthazer ES, Stryker MP (1996) The role of activity in the development of long-range horizontal connections in area 17 of the ferret. *J Neurosci* 16:7253–7269.
33. Hofer SB, Mrsic-Flogel TD, Bonhoeffer T, Hübener M (2009) Experience leaves a lasting structural trace in cortical circuits. *Nature* 457:313–317.
34. Bayer KU, De Koninck P, Leonard AS, Hell JW, Schulman H (2001) Interaction with the NMDA receptor locks CaMKII in an active conformation. *Nature* 411:801–805.
35. Hudmon A, et al. (2005) A mechanism for Ca^{2+}/calmodulin-dependent protein kinase II clustering at synaptic and nonsynaptic sites based on self-association. *J Neurosci* 25: 6971–6983.
36. Shen K, Meyer T (1999) Dynamic control of CaMKII translocation and localization in hippocampal neurons by NMDA receptor stimulation. *Science* 284:162–166.
37. Glazewski S, Giese KP, Silva A, Fox K (2000) The role of α-CaMKII autophosphorylation in neocortical experience-dependent plasticity. *Nat Neurosci* 3:911–918.
38. Wilbrecht L, Holtmaat A, Wright N, Fox K, Svoboda K (2010) Structural plasticity underlies experience-dependent functional plasticity of cortical circuits. *J Neurosci* 30: 4927–4932.
39. Turrigiano GG (2008) The self-tuning neuron: Synaptic scaling of excitatory synapses. *Cell* 135:422–435.
40. McCurry CL, et al. (2010) Loss of Arc renders the visual cortex impervious to the effects of sensory experience or deprivation. *Nat Neurosci* 13:450–457.
41. Gao M, et al. (2010) A specific requirement of Arc/Arg3.1 for visual experience-induced homeostatic synaptic plasticity in mouse primary visual cortex. *J Neurosci* 30: 7168–7178.
42. Zacharias DA, Violin JD, Newton AC, Tsien RY (2002) Partitioning of lipid-modified monomeric GFPs into membrane microdomains of live cells. *Science* 296:913–916.
43. Rizzo MA, Springer GH, Granada B, Piston DW (2004) An improved cyan fluorescent protein variant useful for FRET. *Nat Biotechnol* 22:445–449.
44. Nguyen AW, Daugherty PS (2005) Evolutionary optimization of fluorescent proteins for intracellular FRET. *Nat Biotechnol* 23:355–360.
45. Lim F, Neve RL (1999) Generation of high-titer defective HSV-1 vectors. *Curr Protoc Neurosci* 4.13:11–17.
46. Kwok S, et al. (2008) Genetically encoded probe for fluorescence lifetime imaging of CaMKII activity. *Biochem Biophys Res Commun* 369:519–525.
47. Yu H, Farley BJ, Jin DZ, Sur M (2005) The coordinated mapping of visual space and response features in visual cortex. *Neuron* 47:267–280.
48. Béïque J-C, et al. (2006) Synapse-specific regulation of AMPA receptor function by PSD-95. *Proc Natl Acad Sci USA* 103:19535–19540.